Journal of Alloys and Compounds 502 (2010) 49–53

Contents lists available at ScienceDirect

Journal of Alloys and Compounds

journal homepage: www.elsevier.com/locate/jallcom

Microstructural evolution and mechanical properties of Ti_3SiC_2–TiC composites

WuBian Tian, ZhengMing Sun*, Hitoshi Hashimoto, YuLei Du

National Institute of Advanced Industrial Science and Technology (AIST), 2266-98 Anagahora, Shimoshidami, Moriyama, Nagoya 463-8560, Japan

ARTICLE INFO

Article history:
Received 22 February 2010
Received in revised form 31 March 2010
Accepted 2 April 2010
Available online 22 April 2010

Keywords:
Ti_3SiC_2–TiC composite
Sintering
Mechanical properties
Scanning electron microscopy (SEM)

ABSTRACT

Ti_3SiC_2–TiC composites were fabricated by pulse discharge sintering technique using three different sets of powder mixtures, i.e. Ti/Si/TiC (TC30), Ti/Si/C/TiC (SI30) and Ti/Si/C (TSC30). Based on X-ray diffraction (XRD) analysis and microstructural observations, starting powder reactants were found to have little effect on phase content but strong influence on the microstructure in terms of phase distribution. The phase distribution mainly relies on the heat released from reaction and the liquid phase content formed during sintering. The mechanical properties of the fabricated dense samples demonstrate that more homogeneous phase distribution, available by choosing the starting reactants of SI30, results in higher flexural strength, whereas the Vickers hardness is almost independent of the microstructure. The enhanced flexural strength in sample SI30 sintered at 1400 °C is mainly attributed to the homogeneous TiC distribution in the microstructure.

1. Introduction

Ternary carbide Ti_3SiC_2 belongs to a new system that contains over 60 carbides and nitrides and is abbreviated as $M_{n+1}AX_n$, where $n = 1, 2, 3$, M is an early transition metal, A is an A-group (mostly IIIA or IVA) element, and X is C or N [1]. It exhibits a good combination of versatile properties [1], such as machinability, thermal and electrical conductivity, thermal shock resistance and damage tolerance. Binary carbide TiC is one of the most promising high-temperature structural materials owing to its high modulus (410–510 GPa), high melting point (3067 °C), high hardness (28–35 GPa) and good erosion resistance [2]. Additionally, TiC shows small thermal expansion mismatch [2] and thermodynamic stability [3] with Ti_3SiC_2, suggesting the possibility of developing Ti_3SiC_2–TiC composites for applications as high wear-resistance mold and TiC-based hard materials.

For Ti_3SiC_2–TiC composites, generally in the Ti_3SiC_2-rich side, several kinds of powder mixtures were used in literatures, such as Ti/Si/C with a small amount of Al [4], Ti/Si/TiC [5], TiH_2/SiC/TiC [6,7], Ti_3SiC_2 powders with TiC powders [8], Ti/SiC/C/TiC and TiH_2/SiC/C [9]. In our previous study [10], we fabricated Ti_3SiC_2–TiC composites with 0–90 vol.% TiC from Ti/Si/TiC powder mixtures in the temperature range from 1200 °C to 1400 °C and studied their densification behavior, microstructure and mechanical properties. It was found that the relative densities of composites sintered at 1400 °C are higher than 98%. The hardness of the samples synthesized at this temperature increases linearly with TiC content while the flexural strength increases to a maximum value followed by a decrease with increasing volume fraction of TiC. The microstructure examination demonstrated that the phase distribution of the synthesized composites is inhomogeneous, in which TiC agglomerates are frequently found. Similarly, Ho-Duc et al. [9] found that the agglomerates of TiC particles connect to each other when using TiH_2/SiC/C as starting powders and the phase distribution becomes relatively uniform when sintered from Ti/SiC/C/TiC powder mixture. However, the microstructural evolution mechanism and the relationship between different microstructure and mechanical properties are not elaborated in detail.

As a successive work on Ti_3SiC_2–TiC composites, our initial motivation was to improve the mechanical properties of the composites by optimizing the phase distribution in the microstructure. Emphasis is place on the fabrication and characterization of Ti_3SiC_2–TiC composites by using three kinds of starting powders, i.e. Ti/Si/TiC (TC30), Ti/Si/C/TiC (SI30) and Ti/Si/C (TSC30). Based on optical microscopic observations and thermodynamic analysis, the mechanism responsible for microstructural evolution is proposed. Furthermore, the effect of microstructure on the mechanical properties of Ti_3SiC_2–TiC composite is discussed.

2. Experimental procedures

Starting powder materials used in the present work were titanium (ca. 45 μm, 99.9%), silicon (ca. 45 μm, 99.9%), graphite (ca. 5 μm, 99.7%) and titanium carbide (ca. 1.72 μm, 99%) (all from Kojundo Chemical Lab., Japan). Three kinds of starting powders (Table 1) were weighed according to the target composition of Ti_3SiC_2–30 vol.% TiC and mixed in air by a Turbula shaker mixer for 24 h. The mixed powders were filled in a graphite mold with an inner diameter of 50 mm and then the mold was put into a pulse discharge sintering (PDS) apparatus (PAS-V, Sodick Co. Ltd., Japan). Samples were sintered in vacuum at 1400–1450 °C for 15 min under a pressure of 50 MPa to obtain nearly full density (Table 1). The PDS system was

* Corresponding author. Tel.: +81 52 7367483; fax: +81 52 7367301.
E-mail address: z.m.sun@aist.go.jp (Z. Sun).

0925-8388/$ – see front matter © 2010 Elsevier B.V. All rights reserved.
doi:10.1016/j.jallcom.2010.04.116

Table 1
Summary of starting powders, sintering parameters, phase content, density and mechanical properties of the synthesized Ti_3SiC_2–30 vol.%TiC composites.

Sample ID	Starting powders	Sintering parameters (°C/min/MPa)	TiC content (vol.%)	Measured density (g/cm^3)	Relative density (%)	Vickers hardness (GPa)	Flexural strength (MPa)
TC3040	Ti/Si/TiC	1400/15/50	23.8	4.61	99.9	7.8 ± 0.6	623 ± 19
SI3040	Ti/Si/C/TiC	1400/15/50	23.7	4.59	99.5	7.6 ± 0.7	677 ± 41
TSC3040	Ti/Si/C	1400/15/50	23.0	4.45	96.5	7.0 ± 0.4	523 ± 33
TSC3045	Ti/Si/C	1450/15/50	22.4	4.56	99.0	7.4 ± 0.5	598 ± 55

cooled down to room temperature with a cooling rate of about 100 °C/min after sintering.

The densities of the sintered samples were measured according to the Archimedes principle. The phase contents were determined by an X-ray diffractometer (X'pert, Philips, Netherlands) with Cu Kα radiation at 30 kV and 40 mA at a scanning speed of 0.02°/s. The samples were mechanically polished and etched in a solution of HNO_3:HF:H_2O = 1:1:1 for 5–10 s before optical microscopic observations.

The Vickers hardness was measured using a Vickers indenter (AVK-CO hardness tester, Akashi, Japan) at a load of 300 N for 15 s. At least ten indentations were made for each test. The flexural specimens were cut by an electrical discharge machine from the bulk samples, and then mechanically ground to a dimension of 4 mm × 3 mm × 36 mm with the tensile surface polished down to 1 μm diamond suspension. The mechanical tests were performed with an Instron 8562 universal testing machine with a crosshead speed of 0.5 mm/min. The flexural strength was calculated using the following equation [12]:

$$\sigma = \frac{3F(L-l)}{2bh^2} \quad (1)$$

where F is the applied load, L and l are the outer (30 mm) and inner (10 mm) spans, respectively, b and h are the width (4 mm) and thickness (3 mm) of the specimen.

3. Results

3.1. XRD analysis of synthesized Ti_3SiC_2–TiC composites

XRD patterns of the synthesized Ti_3SiC_2–30 vol.% TiC composites are shown in Fig. 1. The reflections of all samples are indexed as Ti_3SiC_2 and TiC phases. No intermediate phases, such as binary titanium silicides, were detected. This indicates the completion of formation of Ti_3SiC_2 when the sintering temperature reaches 1400 °C or above. Zhang et al. [11,12] reported that the final stage of the Ti_3SiC_2 formation is accomplished by the reactions between the Ti-Si liquid phases and the TiC particles when using Ti/Si/C or Ti/Si/TiC powder mixture. These reactions complete quickly at temperatures higher than 1300 °C, which is consistent with our XRD results. The measured volume fractions of TiC (V_{TC}) in the synthesized Ti_3SiC_2–TiC samples were calculated by the following equations [13]

$$V_{TC} = \frac{I_{TC}/I_{TSC}}{1.95 + I_{TC}/I_{TSC}} \quad (2)$$

where I_{TSC} and I_{TC} are the integrated intensities of the Ti_3SiC_2(1 0 4) and TiC(2 0 0) peaks, respectively. The TiC contents of the synthesized samples are listed in Table 1. Note that the TiC contents for composites TC3040 and SI3040 are very close (23.8% vs. 23.7%), which is slightly higher than that of TSC30 series (22.4–23.0%), suggesting that the starting powders have limited effect on the phase contents. The volume fraction of TiC is, however, lower than the target value, which is also found in our previous study [10], and the reason for this phenomenon is still under investigation.

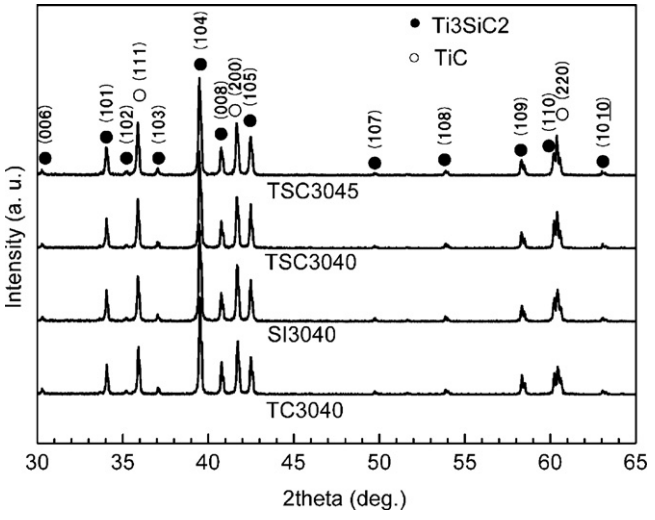

Fig. 1. XRD patterns of sample (a) TC3040, (b) SI3040, (c) TSC3040 and (d) TSC3045.

3.2. Microstructure examinations

Optical microscopic observation results on the etched surfaces of the synthesized Ti_3SiC_2–TiC composites are shown in Fig. 2. The microstructure of composite TC3040 consists of Ti_3SiC_2 grains (in colors) and the TiC grains (white), as shown in Fig. 2(a), in which TiC agglomeration prevails (with indication on micrograph) with elongated Ti_3SiC_2 grains formed around them. On the other hand, a majority of TiC phases distribute uniformly in Ti_3SiC_2 matrix for composite SI3040 (Fig. 2(b)). In composite TSC3040 (Fig. 2(c)), compared with composite TC3040, larger TiC agglomerates were observed, which coexist with Ti_3SiC_2 grains. Note that the grain size of Ti_3SiC_2 phase does not change significantly in the three composites, with comparable size in TC3040 and SI3040 and slightly larger size in composite TSC3040. Apparently, SI3040 shows the most homogeneous phase distribution among the three composites, suggesting that starting powders have strong effect on the microstructure and phase distribution.

3.3. Mechanical properties

The relative density of composite TSC3040 was measured to be 96.5%, relatively lower than the values for composites TC3040 and SI3040 (>99.5%), all sintered at the same temperature of 1400 °C, as shown in Table 1. To compare the mechanical properties of samples with close density, we fabricated Ti_3SiC_2–30 vol.% TiC composite from Ti–Si–C at 1450 °C, i.e. sample TSC3045, whose relative density was measured to be 99.0%.

The Vickers hardness values and flexural strengths of the synthesized composites were measured and listed in Table 1. It is not surprising that the Vickers hardness and flexural strength of composite TSC30 increase with the sintering temperature (comparing TSC3040 and TSC3045) because of the improved density. The hardness values of all the dense composites (i.e. TC3040, SI3040 and TSC3045) locate in the narrow range of 7.4–7.8 GPa. By comparing with the hardness of Ti_3SiC_2–TiC composites containing close TiC contents, we found the values obtained in this study are in good agreement with the data reported by Ho-Duc et al. (8 ± 1 GPa) [9], but are lower than that obtained by Zhang et al. (around 12 GPa) [4].

However, the flexural strength of the composites demonstrates its dependence on the microstructures that are originated from the starting powders. Composite SI3040, with the most uniform microstructure, shows the highest flexural strength with a value

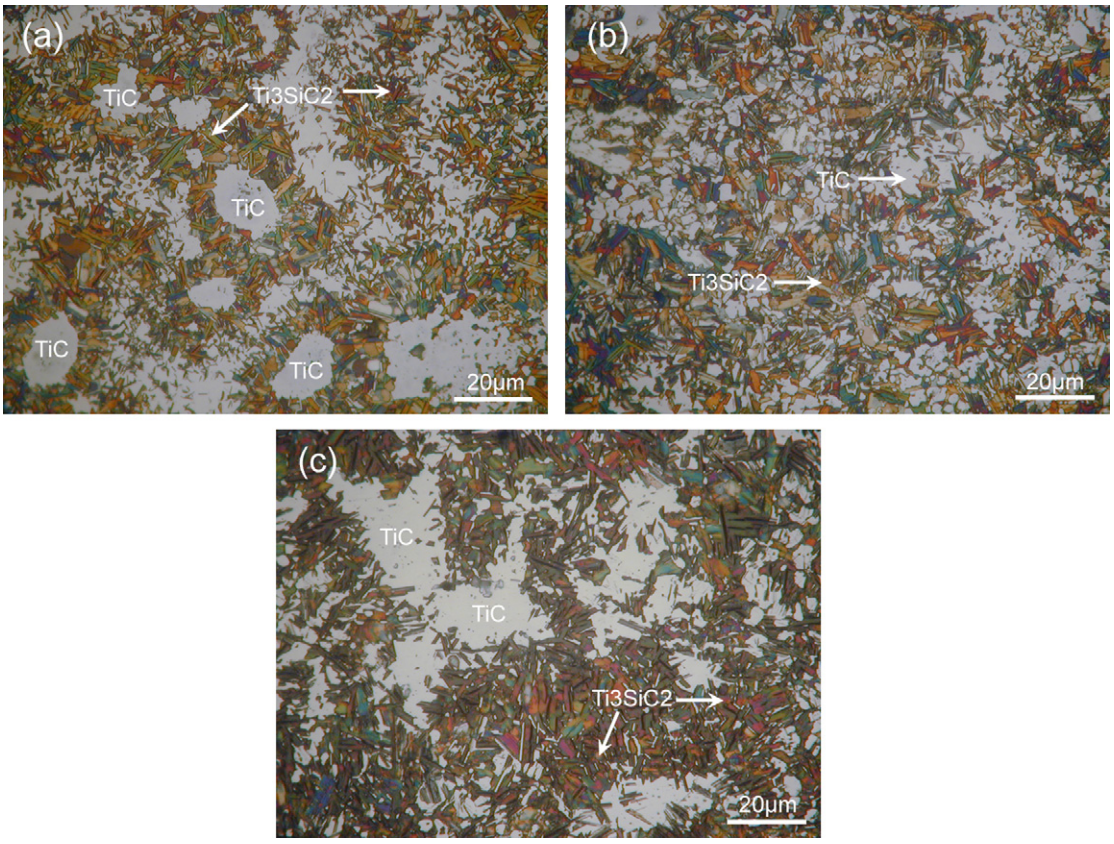

Fig. 2. Optical microscope images on the polished and etched surface of sample (a) TC3040, (b) SI3040 and (c) TSC3040.

of 677 ± 41 MPa, followed by composite TC3040 and then composite TSC3045. The reported flexural strengths of composites with a composition close to Ti_3SiC_2–30 vol.% TiC locate in a range of 365–726 MPa [4,6–9] and our results fall into the range.

4. Discussion

4.1. Microstructure evolution mechanism

It is well understood that the microstructures of reaction synthesized composites are basically influenced by the composition of starting powders and sintering processes [14]. The results of reactive sintering of ZrB_2–SiC composites from a mixture of Zr, Si and B_4C demonstrated that the final microstructure of obtained composite possesses the features of Zr and Si starting powders [15]. In the present study, particle sizes of titanium (45 μm) and silicon (45 μm) are significantly larger than those of TiC (1.72 μm) and graphite (5 μm), easily leading to the agglomeration of finer powders after mixing process. The agglomerates in mixtures will result in non-uniform microstructure after sintering in some cases, such as TC3040 and TSC3040 (see Fig. 2(a) and (c)). Whereas this agglomeration is compromised by the sintering process in SI3040 (Fig. 2(b)), suggesting that the microstructure of composite is further affected by the reaction mechanism and reaction kinetics during sintering.

When sintering Ti_3SiC_2 from Ti/Si/C powder mixtures, Sato et al. [16] proposed that the reaction between Ti and C is triggered firstly to form TiC phase at temperatures higher than 1000 °C, which is a highly exothermic reaction that can increase local temperature inside the powder compacts. Yeh and Shen [17] prepared Ti_3SiC_2 from Ti/Si/C powder mixtures containing different amount of TiC using combustion synthesis. They found that the reaction temperatures for Ti/Si/C elemental powder compacts increase to above 1450 °C abruptly and decrease with increasing TiC content in starting powders, resulting in a reduced amount of liquid phases. We have calculated the enthalpy change of the reactions for 100 g of each starting powder mixture according to thermodynamic data [18–20], assuming that the starting powders completely transfer into intermediate phases:

$$\Delta H^{TC30} = 0.35 \times \left(\frac{1}{7}\Delta H^{Ti_5Si_3} + \frac{2}{7}\Delta H^{TiSi_2}\right) = -42.5\,\text{kJ} \quad (3)$$

$$\Delta H^{SI30} = 0.35 \times \left[\frac{1}{7}\Delta H^{Ti_5Si_3} + \frac{2}{7}\Delta H^{TiSi_2}\right] + 0.70 \times \Delta H^{TiC} = -171.3\,\text{kJ} \quad (4)$$

$$\Delta H^{TSC30} = 0.35 \times \left[\frac{1}{7}\Delta H^{Ti_5Si_3} + \frac{2}{7}\Delta H^{TiSi_2}\right] + 1.23 \times \Delta H^{TiC} = -268.8\,\text{kJ} \quad (5)$$

Obviously, all the reactions are exothermic and the released heat during sintering is the lowest in TC30 and the highest in TSC30. The difference is due to the varied amount of TiC, which starts to form at around 1000 °C and provides the energy for eutectic reaction in Ti-Si system. Accordingly, the content of liquid phase formed during sintering is the lowest in TC30 and the highest in TSC30 with SI30 in between. The strong exothermic heat results in the abrupt shrinkage of displacement starting at 1160 and 1200 °C for sample SI3040 and TSC3040, respectively, as indicated in Fig. 3. This shrinkage corresponds to the sudden increase in temperature and the formation of liquid phases. Note that the shrinkage of TC3040 starting at 1330 °C agrees well with the eutectic point of titanium silicide compound.

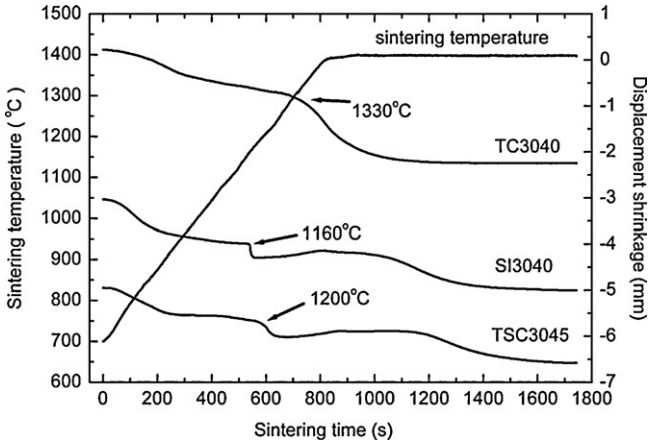

Fig. 3. Variation of shrinkage of displacement and sintering temperature with sintering time.

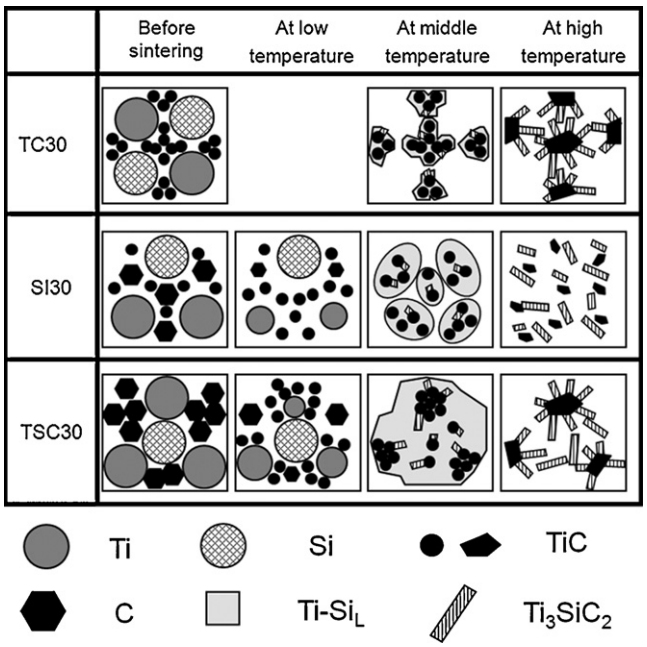

Fig. 4. Schematic diagram of microstructural evolution from powder mixtures of TC30, SI30 and TSC30. The temperature varies in horizontal direction in sequence of before sintering, at low temperature, at middle temperature and at high temperature.

Based on the results above, we have proposed the schematic diagrams of microstructural evolution during sintering when starting from three different powder mixtures, as illustrated in Fig. 4. In composites SI3040 and TSC3040, TiC phase is formed firstly by the combustion reaction between Ti and C at temperatures above 1000 °C. Reaction heat releases simultaneously and triggers the reactions of the formation of Ti–Si liquid phases. While in composite TC3040, the Ti–Si liquid reactions occur at the binary eutectic temperature. The microstructural uniformity relies on not only the characteristic of starting powders but mainly the heats of reaction and the liquid phase content formed during sintering. The non-uniform microstructures observed in the two composites of TC3040 and TSC3040 are predominantly attributed to inappropriate amount of Ti–Si liquid phases formed during the reactive sintering process, with too small amount in the case of TC3040 and too much in TSC3040. When the amount of Ti–Si liquid phase is too little, TiC agglomerates are not wetted thoroughly and Ti_3SiC_2 is formed around TiC particles (TC30 in Fig. 4). When there is too much liquid phase, however, TiC partially dissolves into the Ti–Si liquid phase and then Ti_3SiC_2 forms and grows up in the areas rich in liquid phase (TSC30 in Fig. 4). The uniform microstructure obtained in composite SI3040 is believed to originate from the appropriate amount of liquid phase formed during sintering (SI30 in Fig. 4).

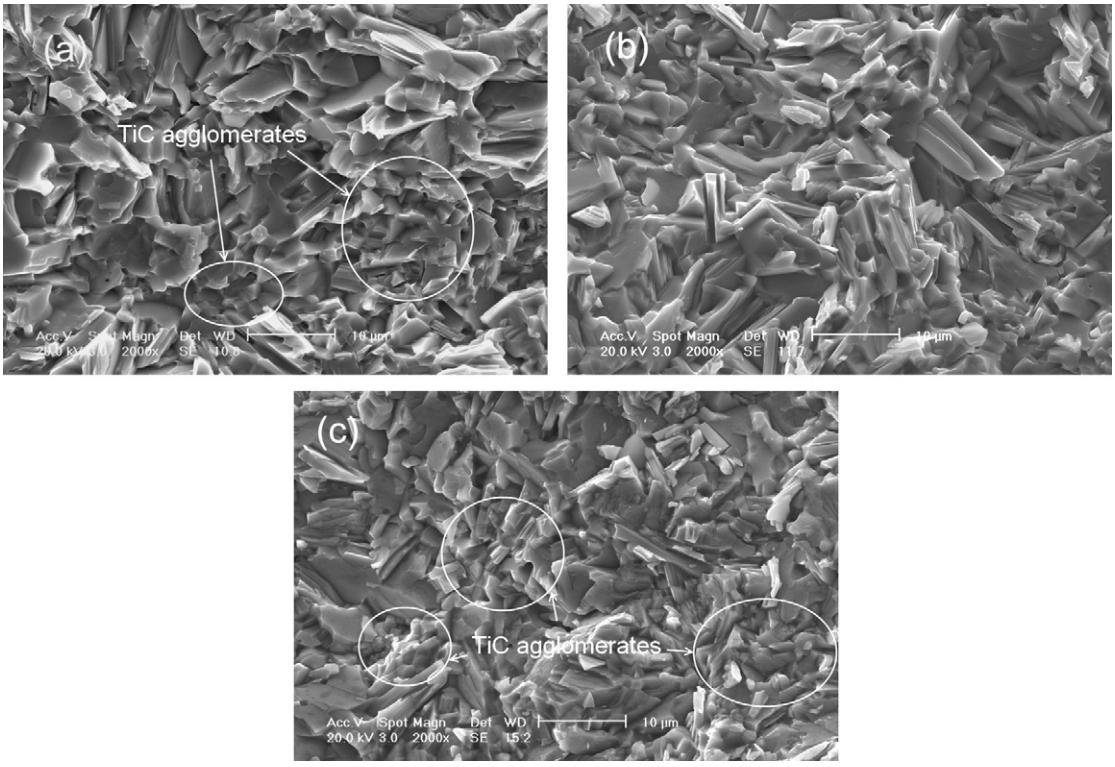

Fig. 5. The fracture surfaces of tested composites (a) TC3040, (b) SI3040 and (c) TSC3040.

4.2. Effect of microstructure on mechanical properties

The fracture surfaces of tested Ti_3SiC_2–TiC composites are shown in Fig. 5, in which all the fracture surfaces consist of predominantly transgranular fracture of Ti_3SiC_2 grains, displaying the layered microstructure and cleavages, and the intergranular fracture of TiC grains. While the optical images show some large TiC agglomerates in composite TC3040 and TSC3045 (Fig. 2(a) and (c)), fracture surface micrographs demonstrate clearly that these agglomerates are composed of small TiC grains with close particle sizes (indicated in Figs. 5(a) and (c)).

Although the hardness values of the three composites are very close, the limited difference can be traced back to the properties of specimens, such as phase constituent, density and microstructure. For example, the slightly higher hardness of TC3040 could be attributed to the relatively higher TiC content and density (Table 1). In addition, hardness generally shows reverse relationship with grain size according to the Hall–Petch relation [21]. Based on microstructural observations, it is found that the dense Ti_3SiC_2–TiC composites show similar grain size of Ti_3SiC_2 phase and TiC phase (Fig. 2 and Fig. 5). Therefore, the grain structures have limited effect on hardness properties. Furthermore, one should be noted that the high indentation load used for hardness test results in large indentation sizes (>250 μm), which are obviously larger than the grain size of Ti_3SiC_2 phase (<10 μm) and even that of TiC agglomerates (<30 μm). In other words, the hardness values measured in this way well represent the average of the microstructure. Consequently, the measured hardness is not sensitive to the uniformity of microstructure.

Mechanical strength of a material is its ability to withstand an applied stress without failure, which mainly relies on its microstructure. We believe that the abovementioned factors affecting hardness property also influence strength. For instance, the higher strengths of TC3040 and SI3040 over TSC3040 are partially associated with the relatively higher TiC content and density. This is because TiC phase usually enhances the mechanical strength of Ti_3SiC_2–TiC composites containing up to 46% TiC in TC series [10] and as high as 30% TiC in previous publication [4], and less pore defects exist in denser composite.

On the other hand, when a composite is cooled down from the fabrication temperature, thermal residual stress arises due to the thermo-elastic mismatch between constituents [22]. The magnitude and distribution of residual stress are influenced significantly by the microstructural features of the composite [9,23]. In the present work, the residual stresses in Ti_3SiC_2 and TiC phase are assumed to be tensile and compressive, respectively, according to the difference of their coefficients of thermal expansion (CTEs) (the CTEs of Ti_3SiC_2 and TiC are 9.1×10^{-6}/K and 7.4×10^{-6}/K, respectively). The coarser TiC agglomerates in TSC30 would result in larger thermal stress, which subsequently weakens the fracture strength of composite. The strongest sample, therefore, is the composite consisting of the finest TiC phase agglomerates, i.e. SI3040. Similar phenomena were also found in Ti_3SiC_2–SiC [9] and Al_2O_3–ZrO_2 composites [22].

5. Conclusions

Three starting powder mixtures, Ti/Si/TiC (TC30), Ti/Si/C/TiC (SI30) and Ti/Si/C (TSC30), were used for the synthesis of Ti_3SiC_2–30 vol.% TiC composites by PDS technique. Based on XRD results and optical microscopic observations, we find that starting powders affect slightly on phase content but significantly on the uniformity of phase distribution, in which SI3040 shows the best uniformity of phase distribution among three composites. The hardness of dense samples (i.e. TC3040, SI3040 and TSC3045) locates in the narrow range of 7.4–7.8 GPa and is not sensitive to microstructure. Sample SI3040 shows the highest flexural strength with a value of 677 MPa followed by sample TC3040 and then sample TSC3045. The variation in flexural strength of the composites is closely associated with the microstructure.

References

[1] M.W. Barsoum, T. El-Raghy, J. Am. Ceram. Soc. 79 (1996) 1953–1956.
[2] H.O. Pierson, Handbook of Refractory Carbides and Nitrides: Properties, Characteristics, Processing and Applications, Noyes Publications, Westwood, New Jersey, 1996.
[3] W.J.J. Wakelkamp, F.J.J. Van Loo, R. Metselaar, J. Eur. Ceram. Soc. 8 (1991) 135–139.
[4] J.F. Zhang, L.J. Wang, W. Jiang, L.D. Chen, Mater. Sci. Eng. A 487 (2008) 137–143.
[5] S. Tada, K. Murase, H. Hashimoto, Z.M. Sun, Mater. Trans. 48 (2007) 139–142.
[6] S. Konoplyuk, T. Abe, T. Uchimoto, T. Takagi, Mater. Lett. 59 (2005) 2342–2346.
[7] S. Konoplyuk, T. Abe, T. Uchimoto, T. Takagi, J. Mater. Sci. 40 (2005) 3409–3413.
[8] J. Lis, L. Chlubny, M. Lopacinski, L. Stobierski, M.A. Bucko, J. Eur. Ceram. Soc. 28 (2008) 1009–1014.
[9] L.H. Ho-Duc, T. El-Raghy, M.W. Barsoum, J. Alloys Compd. 350 (2003) 303–312.
[10] W.B. Tian, Z.M. Sun, H. Hashimoto, Y.L. Du, Mater. Sci. Eng. A 526 (2009) 16–21.
[11] Z.F. Zhang, Z.M. Sun, H. Hashimoto, T. Abe, J. Alloys Compd. 352 (2003) 283–289.
[12] Z.F. Zhang, Z.M. Sun, H. Hashimoto, T. Abe, J. Eur. Ceram. Soc. 22 (2002) 2957–2961.
[13] Z.M. Sun, Z.F. Zhang, H. Hashimoto, T. Abe, Mater. Trans. 43 (2002) 428–431.
[14] G.J. Zhang, M. Ando, J.F. Yang, T. Ohji, S. Kanzaki, J. Eur. Ceram. Soc. 24 (2004) 171–178.
[15] G.J. Zhang, Z.Y. Deng, N. Kondo, J.F. Yang, T. Ohji, J. Am. Ceram. Soc. 83 (2000) 2330–2332.
[16] F. Sato, J.F. Li, R. Watanabe, Mater. Trans. 41 (2000) 605–608.
[17] C.L. Yeh, Y.G. Shen, J. Alloys Compd. 458 (2008) 286–291.
[18] J.A. Dean, Lange's Handbook of Chemistry, McGraw-Hill, New York, U.S.A., 1999.
[19] D.P. Riley, C.P. Oliver, E.H. Kisi, Intermetallics 14 (2006) 33–38.
[20] M. Doyama, M. Yabe, Data Handbook of Intermetallic Compounds Science Forum, Tokyo, 1989.
[21] R.W. Rice, C.C. Wu, F. Borchelt, J. Am. Ceram. Soc. 77 (1994) 2539–2553.
[22] J.F. Bartolomé, G. Bruno, A.H. DeAza, J. Eur. Ceram. Soc. 28 (2008) 1809–1814.
[23] P. Agrawal, K. Conlon, K.J. Bowman, C.T. Sun, F.R. Cichocki, K.P. Trumble, Acta Mater. 51 (2003) 1143–1156.